The Translational and Rotational Dynamics of Cigar-Shaped Colloid Particles

Magdalena Kordon
Alexander Schavkan

September 9, 2009

Supervisor: Christian Gutt
Adviser: Birgit Fischer and Fabian Westermeier
Adviser at beamline: Wojciech Roseker and Jan Perlich
Adviser in synthesis:Alexander Kadenkin

Contents

List of Figures

1 Introduction

Colloids are suspensions in which small particles are dispersed evenly throughout a liquid. In contrast to a solution they are not completely dissolved. The size of the suspended particles is in μm - nm range. They are small enough to be dispersed evenly and maintain a homogenous appearance, however, on the other hand large enough to scatter light. Suspensions are present in various systems of scientific and technological importance, such as paints, ceramics, cosmetics, agricultural sprays, detergents, soils, biological cells and in food industry. In science colloids are investigated for example to find the explanation of phase behavior, glass transition, diffusion and the dynamics of these systems. Many various interactions can be observed between the colloidal particles, such us the excluded volume repulsion, electrostatic interaction, van der Waals, entropic and steric forces. In order to avoid agglomeration of particles one should stabilize them. Firstly it is possible to attain the steric stabilization by covering the surface of the particles with a polymer layer which causes an entropic repulsive force. Secondly we can screen the surface by adding salt which lessens the potential. In order to stabilize the particles we need surface charge so that the particles do not come too close to each other.

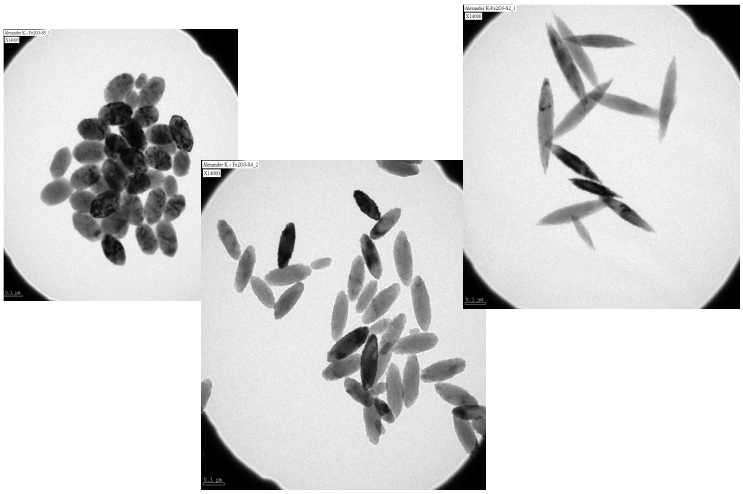

Figure 1: TEM images of cigar-shaped particles with different aspect ratio (Hematite a-Fe_2O_3):the cigar-shaped particles which are not covered with a siliciumdioxide layer have much sharper edges

In our experiment we focused on a very specific colloidal system consisting of cigar-shaped particles (particles with approximately the shape of a prolate

ellipsoid). In this kind of a system the interactions and the dynamics are much more complicated than in the case of round particles. Not only should we take the translation into account when considering the Brownian motion but also the rotational movement. Both rotation and translation are present in the case of round and elliptical particles. However, the shape and the symmetry of the round particles disables us to see any changes in the effect of scattering light caused by rotation. We are only able to observe the translational movement. Whereas in the case of cigar-shaped particles both types of diffusion have the contribution into the light scattering and the polarization of the light.

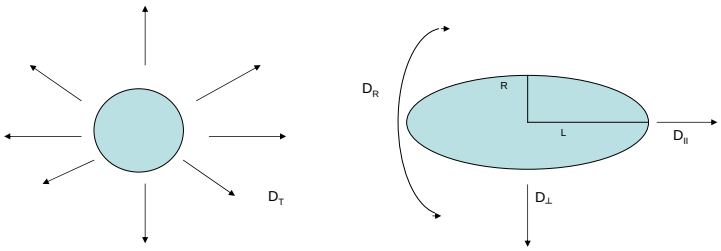

Figure 2: The difference in diffusion between round and cigar-shaped particles

2 Theory

Scattering is the general process of interaction of radiation with her environment. Not only is the light scattering effect the essential reason why people are able to see the world but it is also one of the basic methods used for investigating the environment and therefore making some progress in science.

2.1 Scattering Theory

If a plane electromagnetic wave passes over an obstacle, charges in the obstacle are set into motion and radiate secondary waves in all directions. The phenomenon is called *scattering*. Generally the term scattering is used when small particles are involved, especially when they are randomly arranged in space.

Let a nearly unidirectional beam having some small cross section and transporting power P be incident on a region containing matter in any form. If the matter is removed, the beam continues undisturbed and defines a forward direction. A detector, located in this direction measures the power P. When the matter is in the place, the same detector measures the power P´ which is always less than P. In this case of extinction of the incoming beam the power $P - P'$ was lost from the incoming beam. The lost part is generally divided in two parts. One is the power in a scattered wave radiating in various directions from the irradiated region of the matter, and the other is a generation of heat through some mechanism of conversion in the interior of the matter called absorption. Extinction may be total and consist almost entirely of absorption or almost entirely of scattering.

When a wave of frequency ω falls on the single atom, the electric field in the former acts on the elastically bound electrons in the latter and sets them into sinusoidal oscillation with the same frequency ω. Each of the electrons acquires the certain instantaneous dipole moment with respect to its position of equilibrium, and as long as scattered wave is concerned, the atom can be regarded as a single dipole whose moment is the vectorial sum of those of the several electrons.

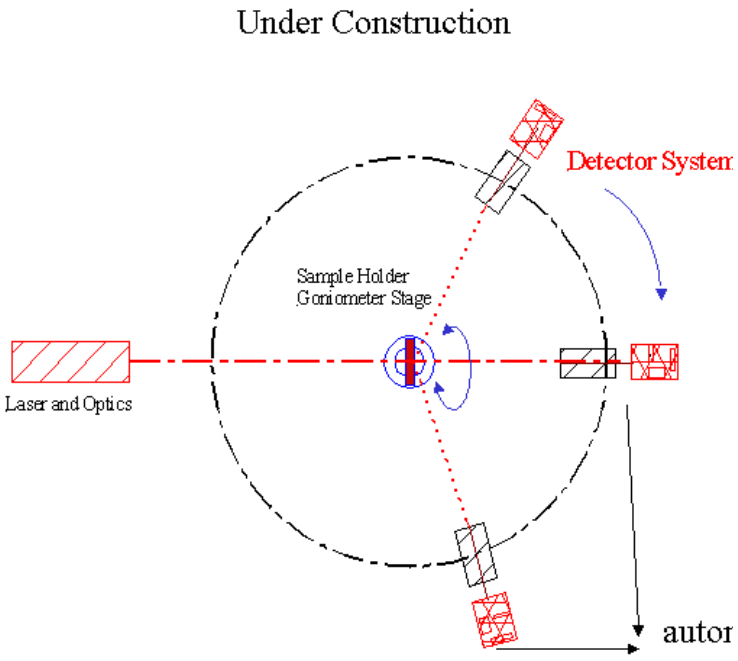

Figure 3: The scheme of light scattering experiment

2.2 Dynamic Light Scattering

2.2.1 Theory of DLS for our Experimental setup

In a light scattering experiment, monochromatic beam of laser light passes through a polarizer to define the polarization of the incident beam and then impinges on a sample. The scattered light then passes through an analyzer which selects a given polarization and finally enters the detector. The position of the detector defined by a scattering angle Θ. In the light scattering experiments is common to use q, which is given by equation 1 istead of Θ.

$$q = \frac{4\pi n}{\lambda} \cdot sin(\theta/2) \tag{1}$$

The intersection between the incident beam and the scattered beam defines the volume V, called the scattering volume or the illuminated volume. In an idealized light scattering experiment the incident light is a plane electromagnetic wave:

$$E_i(r,t) = n_i E_0 e^{i(\mathbf{k}_i \cdot \mathbf{r} - \omega_i t)} \qquad \text{with} \tag{2}$$

λ - wavelength
ω_i - frequency
n_i - polarization
$E - 0$ - amplitude
k_i - wave vector

$$k_i = \left(\frac{\omega_i}{c}\right) \hat{\mathbf{k}}_i \tag{3}$$

$\hat{\mathbf{k}}_i$ is the unit vector specifying the direction of propagation of the incident wave. $E_i(r,t)$ is the electric field at the point in the space $\mathbf{r}$ at time t. The charges of particles in the illuminated volume experience the force by this incident electric field and are accelerated. Accelerated charges radiate light - this scattered light field is the sum of the all electric fields, which are radiated by all the charges in the scattering volume and arrive at the detector. That radiate field depends on the exact positions of the charges. The particles have different number of degrees of freedom - so they can move, rotate and/or vibrate. Because of this motion the positions of the particles are constantly changing and the electric field, which arrive at the detector will fluctuate in time. It is possible to get important structural and dynamical information about the position and orientation of the particles from this fluctuations. To get that information from fluctuations of the scattered electric field you can use correlation functions. Correlation functions provide a concise method for expressing the degree to which two dynamical properties are correlated over a period of time. If several particles are supposed to have a property A, which depends on the positions and momenta of the particles in the system, which

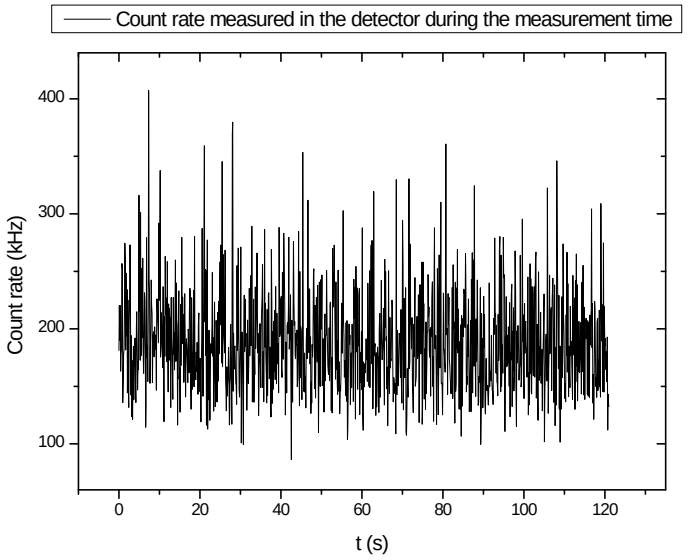

Figure 4: The fluctuation of intensity

are depending from time, the property A will change in time depending on the motion of the particles. Even, when the particles are moving according to e.g. Schrödinger´s equation, their huge amount makes their motion random, so the dependence of property A will generally resemble a noise pattern (see Fig. 4.

The autocorrelation function (equation 4 can be calculated from this pattern.

$$\langle A(0)A(\tau)\rangle = \lim_{T\to\infty} \frac{1}{T} \int_0^T dt A(t)A(t+\tau) \tag{4}$$

After normalization this function will look like equation 5

$$g^{(2)}(\tau) = \langle I(t)I(t+\tau)\rangle \,/\, \langle I\rangle^2 \tag{5}$$

The time correlation function of a nonperiodic property A decays from $\langle I^2\rangle$ to $\langle I\rangle^2$ in the course of time. So $g^{(2)}(\tau)$ can be written in dependence of Γ like in equation 6.

$$g^{(2)}(\tau) - 1 = Ae^{-2\Gamma\tau} \tag{6}$$

Γ can be calculated from the equation 6 and from Γ it is possible to get the parameters of the particles in the sample.

2.2.2 Experimental Setup

In the DLS method a 30mW 632.8 nm He-Ne laser is used as a light source. In order to adjust the intensity coming into the detector the setup is equipped with several absorption filters located in two rotating wheels. Each filter has a different optical density value. Then the beam goes towards the beam-splitter where its intensity is measured by a photo diode before it is split into two beams. This cleavage is essential in making the cross-correlation possible as it lets decrease the contribution of multiple scattered light to the data measured in the detector. Afterwards the light is filtered on the first polarizer what makes us sure that there is only one direction of polarization. Then two polarized laser beams are focused by the lens system so that the light can go through a quartz capillary filled with the sample.

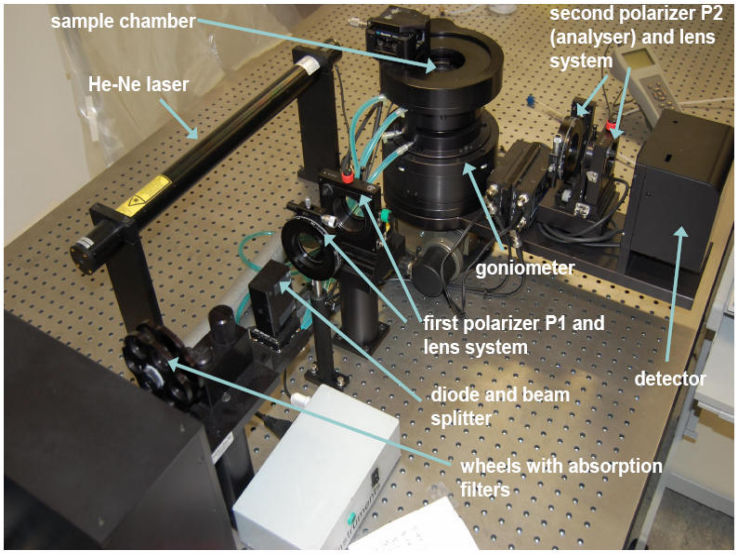

Figure 5: The setup of the dynamic light scattering experiment

The capillary is placed in the chamber with a temperature regulating system. All the measurements have been carried out at 20°. The sample chamber is located above a goniometer which is connected to the detector. The goniometer is able to change the value of the scattering angle from 30° to 150°. The particles in the sample are responsible for scattering the light. The scattered beams initially go through the second polarizer (analyzer), then through another lens system and finally they reach the detector where the intensity is measured. There is another important part of the equipment which is a correlator. This is a small box situated under the table where the auto-correlation function $g_2(q,t) - 1$ is calculated from the data collected on the detector. As a matter of fact the auto-correlation function and the

intensity of light are the most important parts of all the following data analysis.

3 Synthesis

The method of the synthesis of cigar-shaped particles that we used had been previously presented in the article by M. Osaki at al [4]. The synthesis was carried out as follows. First we added 2.7 g of $FeCl_3$ o $6H_2O$ to 0.5 l of deionised water. In order to get the elliptical shape of the particles we had to add an adequate concentration of NaH_2PO_4 (around 4.5 mM) ie 35.1 mg. NaH_2PO_4 is responsible for blocking two axis so that the particles grow only in one direction becoming more and more elliptical in shape. NaH_2PO_4 determines the ratio between the length and the width of the particles. After adding all the aducts mentioned above we stirred the mixture for two days at 100°C under reflux. During this process the hematite particles were formed. We could observe it in a change of color from yellow to orange. The precipitate was then repeatedly centrifuged and washed with distilled water to remove all extraneous ions. Then it was resuspended in ethanol and filtered. As a result we obtained hematite particles, a-Fe_2O_3, in ethanol.

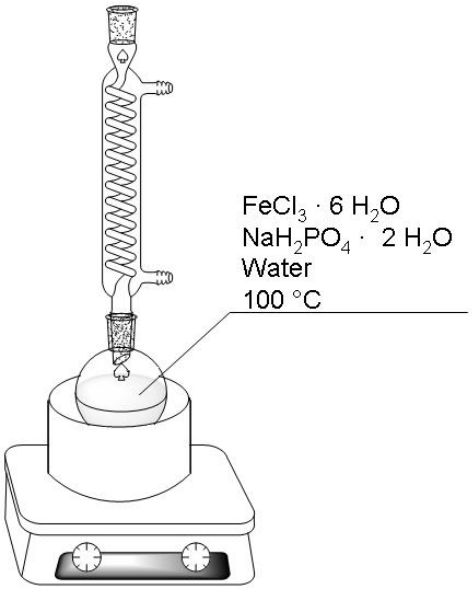

Figure 6: The scheme of synthesis equipment

In order to stabilize the particles with a polymer layer we used polyvinylpyrrolidone (PVP). First we added a very small amount of PVP and left the mixture stirring for about 24h. Next the samples were centrifuged and washed with ethanol in order to remove the excess of PVP. The following step was to cover them with a siliciumdioxid. Therefore we add 25 % ammonium-hydroxide and tetraethoxysilane TEOS and leave it stirring for 24h to cover the particles with a thin silicium-dioxide shell. The final aim was to disperse the particles in Dibutylphthalate. However, to do that we had to add Tripropy-

lmethacrylate (TPM) to this reaction after a day to lessen the polarity of the surface of the particles. The samples were stirred again for another 24h. Then we removed ammonium-hydroxide using a rotary evaporator and the samples were centrifuged and redispersed in ethanol twice. In the end we could disperse the particles in Dibutylphthalate.

4 Results

4.1 Verification of Linear Polarization of Laser Light

The linear polarization of the laser light was verified by the experiment carried out only with polarizer 1, which is positioned after the beam splitter and before the sample. We got a sinus curve of intensity of the scattered light in case of round particles and sinus curve with different parameters in case of cigar-shaped particles as a result. The reason for such a shape of the curve is that if we have maximal amount of light going through the polarizer at one point and we change the angle of this polarizer to the value 90° smaller or larger we will get the minimal amount of light going through. The example of cigar-shaped particles (Fig. 7) let us see the clear difference between maxima and minima in the plot.

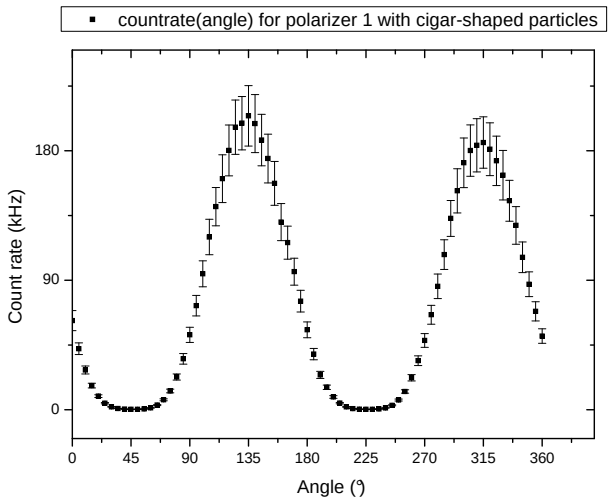

Figure 7: Intensity plot of scattered light over angle of polarizer 1

4.2 Verification of Changes of Polarization of the Laser Light after Scattering from the Samples

We set the polarizer 1 to maximum at 317,5° in order to have linearly polarized light and added the polarizer 2 (analyzer) to the set up. The theoretical prediction was, that scattering light on round particles would change the angle of the linear polarization of laser light. In the case of round particles it is only possible to observe the translational movement. The rotation of round particles is present, too, but we could not see it, because of the spherical symmetry of the rotational tensor. As we can see we managed to detect the minimum at 90° difference to the maximum like we expected. After all the measurements we could see that the angle of polarization of the light changed after having been scattered on the sample. We did the same measurement with the cigar-shaped particles. Due to the anisotropic change the linearly polirized light will alter the polarization. We expect that we do not get a minimum there the intensity is really zero. The results are displayed in the Fig. 8 and 9.

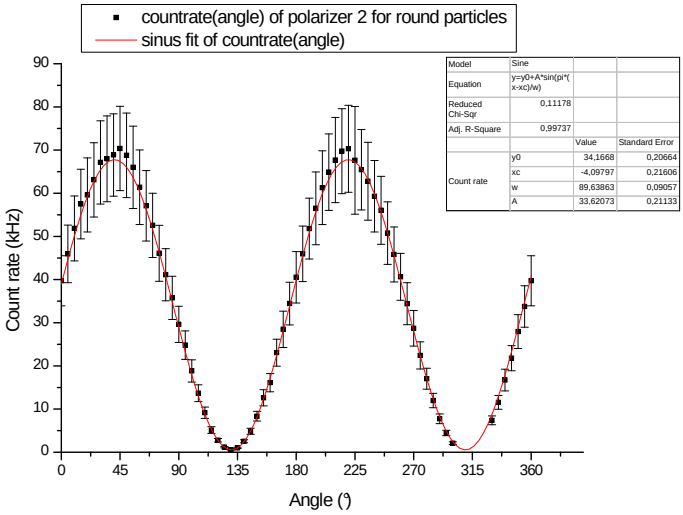

Figure 8: Intensity plot of scattered light over angle of polarizer 2 for sample with round particles

In both cases we obtained sinus curves. The comparison of these plots showed in the first case the difference between the minimum for round particles and the minimum for cigar-shaped particles, like assumed the minimum value is higher for cigar-shaped particles. This difference is presented in Fig. 10.

The difference was interpreted as an evidence of rotational movement. We assumed that in the maximum the translational movement is dominant because most of scattered light goes through the analyzer, so we cannot

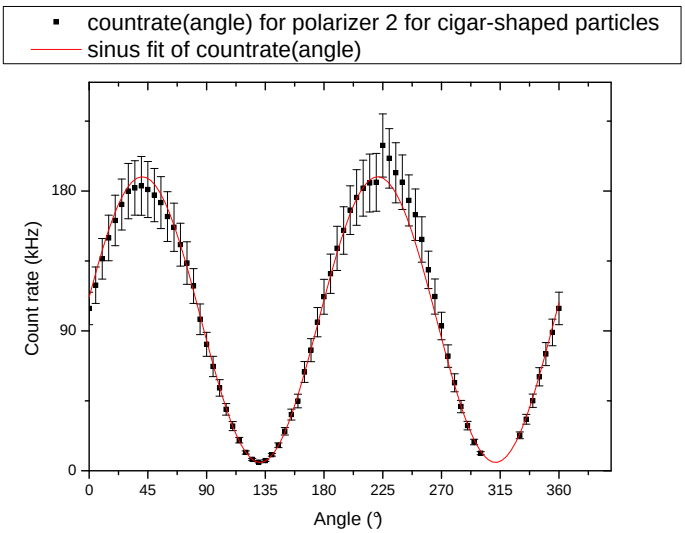

Figure 9: Intensity plot of scattered light over angle of polarizer 2 for sample with cigar-shaped particles

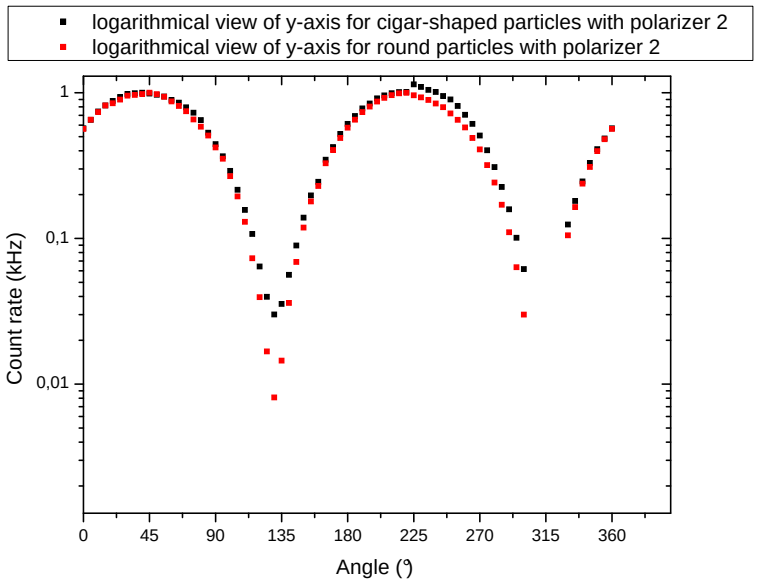

Figure 10: Comparison of the sinus diagrams from the measurement with polarizer 1 set to the maximal intensity and the angle of polarizer 2 changed from 0° to 360° for round and cigar-shaped particles with the y-axis put in a logarithmical scale

observe the rotation and any difference in the curve representing round or cigar-shaped particles. In the minimum only the components of elliptically

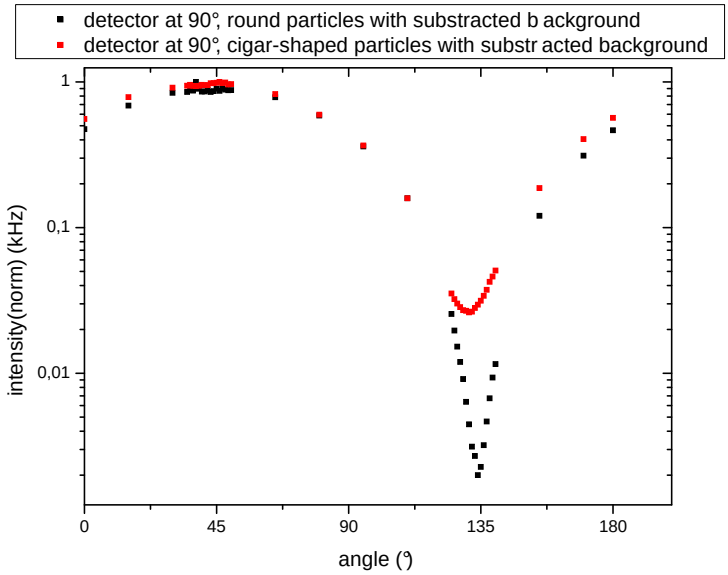

Figure 11: Comparison of the sinus diagrams from the measurement with polarizer 1 set to the maximal intensity and the angle of polarizer 2 changed from 0° to 360° for round and cigar-shaped particles with the y-axis put in the logarithmical scale with light scattering angle of 90°

polarized light can go through the analyzer, so we can see the intensity for round particles at zero (or almost zero because there is always some background calculated) and the intensity for cigar-shaped particles on constant value, which is coming from the rotational movement.

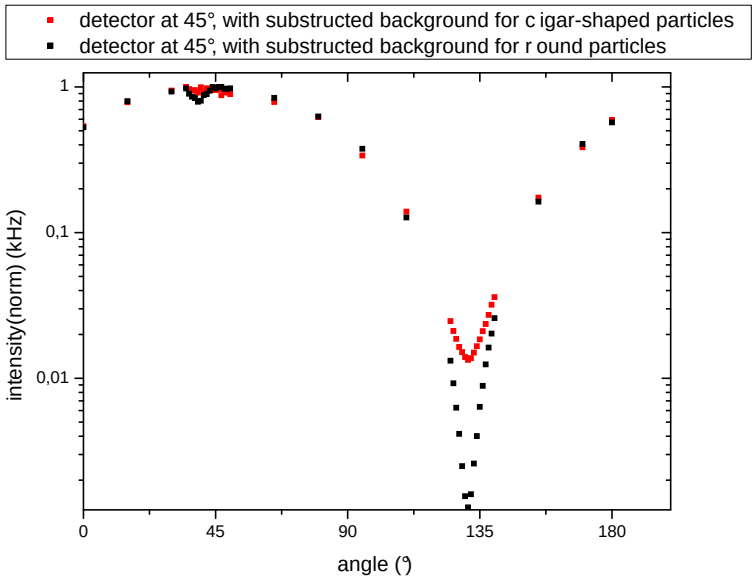

Figure 12: Comparison of the sinus diagrams from the measurement with polarizer 1 set to the maximal intensity and the angle of polarizer 2 varied from 0° to 360° for round and cigar-shaped particles with the y-axis put in the logarithmical scale with light scattering angle of 45°

We verified this assumption by scattering the light with the value of scattering angle of 90° and 45° (the change of scattering angle means the change of the detector position) and measured the areas near maximum and minimum more precisely. The results are illustrated in the Fig. 11 and 12.

This measurement approved our assumption.

4.3 Prospects and Results of Measurements

We expected that after the measurement of autocorrelation function and calculation of $\Gamma(q^2)$ for different q´s we will get a straight line, which would intercept the y-axis in zero. For the plot of $\Gamma(q^2)$ from cigar-shaped particles we assumed, that the interception point would be shifted by constant value and from this value we could calculate the q^2 independent constant coefficient of rotational movement. The graphical demonstration of our assumption is illustrated in the Fig. 13

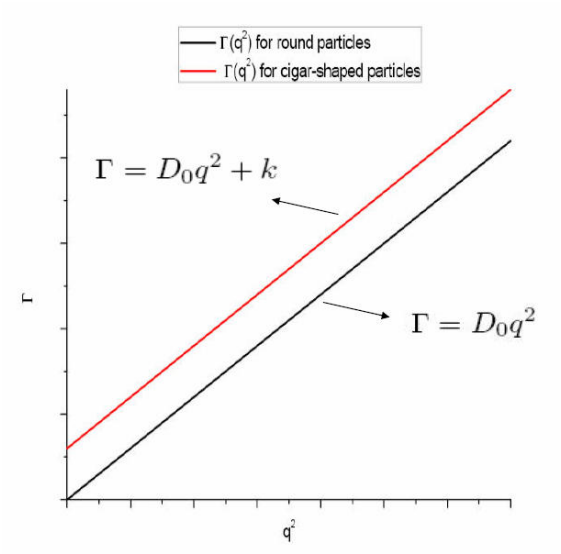

Figure 13: Expected dependence $\Gamma(q^2)$ for round and cigar-shaped particles

We measured the autocorrelation functions for round particles at different scattering angles from 40° to 140° and calculated $\Gamma(q^2)$ for the setups with analyzer set to maximal intensity passing through and minimal intensity passing through. The results are demonstrated in the figures 14, 15, 16.

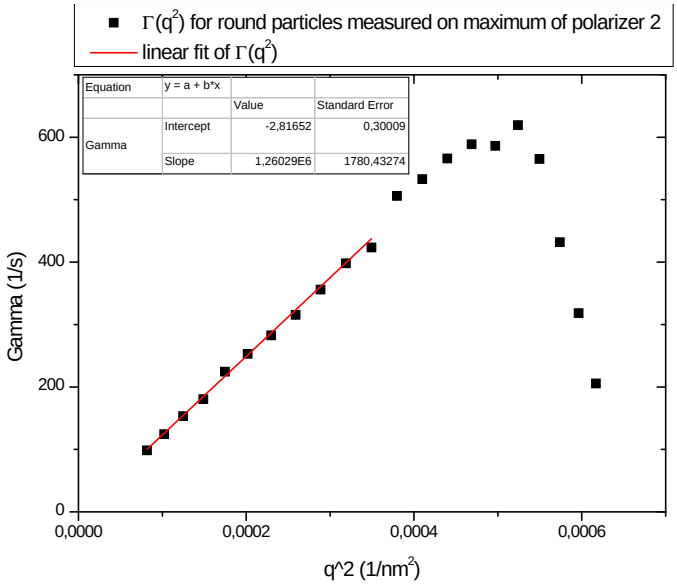

Figure 14: Plot of $\Gamma(q^2)$ for round particles measured with analyzer set to maximal intensity detected

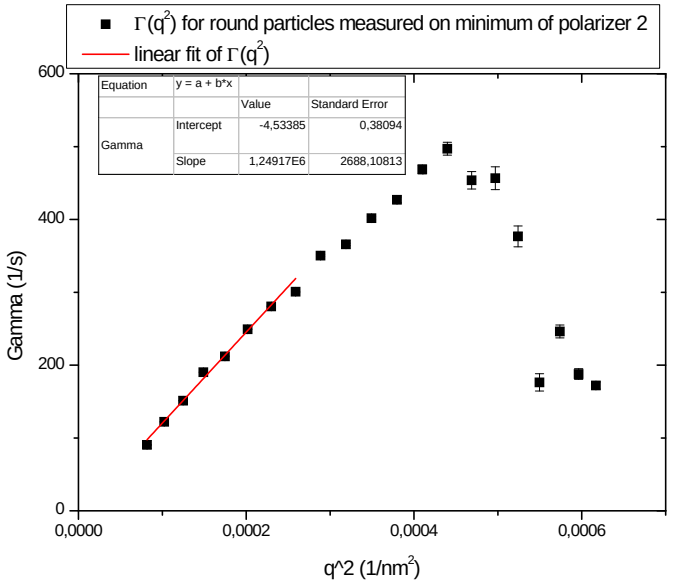

Figure 15: Plot of $\Gamma(q^2)$ for round particles measured with analyzer set to minimal intensity detected

We assumed that the rotation of cigar-shaped particles does not depend on q and that is why this component shifts the function. Γ-function will be

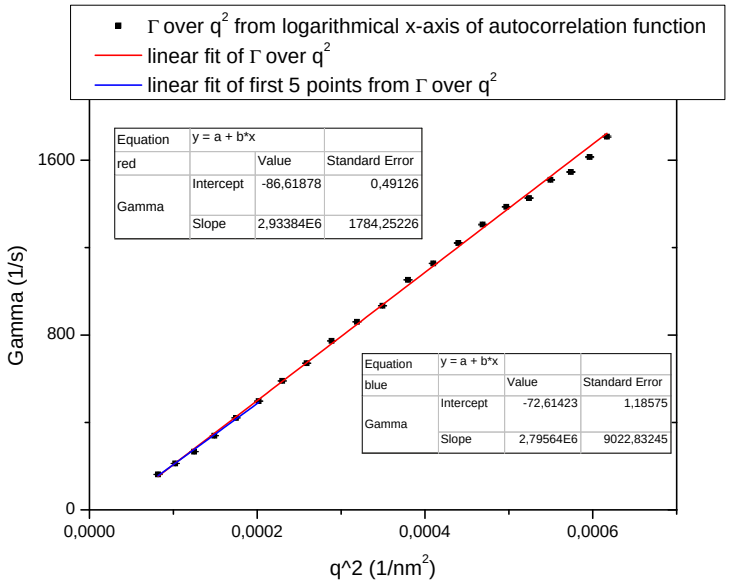

Figure 16: Plot of $\Gamma(q^2)$ for cigar-shaped particles measured with analyzer set to maximal intensity detected

shifted by this value. To get the plots we used equation 6. From this equation we got the values for $\Gamma(q^2)$, which we plotted. The plots from round particles were intercepting the zero point with error of ± 5. The interception point of plots for cigar-shaped particles was between -33 and -218. It was depending from the quality of evaluation and error bars. The Fig. 16 is one example for evaluation of the $\Gamma(q^2)$-plots for cigar-shaped particles. The intensity in the measurements of round particles was too low for higher qs, so Γ-values dropped. In these two measurements we only could use the first 9 and 11 points to fit the curve and calculate the interception point.

5 Conclusions and Outlook

The DLS method let us confirm the presence of both translation and rotation of the particles in the colloidal systems. What we could find was the size and the diffusion constants. What is more, all the results show how big is the influence of symmetry on the dynamics of the whole system. We know for sure that there are differences between round and cigar-shaped particles. We saw them in our experiment and in our evaluation. But so far we have not been able to calculate the parameters of cigar-shaped particles. We made the same measurements for the cigar-shaped particles.

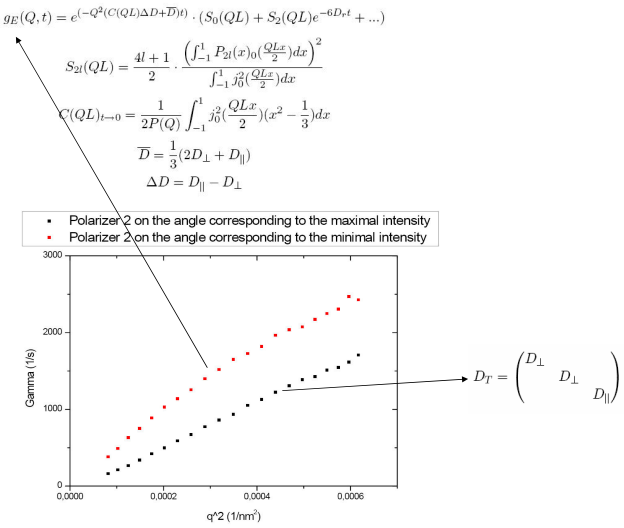

Figure 17: Plots of $\Gamma(q^2)$ for cigar-shaped particles measured with analyzer set to maximal and minimal intensity detected and the theory equations, which we used

At minimum of polarizer 2 the Γ is shifted and the is a slight curve visible. We should compare our results to the theory. In the last step of our research we tried to compare our plots to the theoretical one.

$$g_E(Q,t) = e^{(-Q^2(C(QL)\Delta D+\overline{D})t)} \cdot (S_0(QL)+S_2(QL)e^{-6D_r t}+...) \qquad \text{with} \quad (7)$$

$$S_{2l}(QL) = \frac{4l+1}{2} \cdot \frac{\left(\int_{-1}^{1} P_{2l}(x) \cdot j_0(\frac{QLx}{2})dx\right)^2}{\int_{-1}^{1} j_0^2(\frac{QLx}{2})dx}$$

$$C(QL)_{t\to 0} = \frac{1}{2P(Q)} \int_{-1}^{1} j_0^2(\frac{QLx}{2})(x^2 - \frac{1}{3})dx$$

$$\overline{D} = \frac{1}{3}(2D_\perp + D_\parallel)$$
$$\Delta D = D_\parallel - D_\perp$$

On the Fig.17 we could see the curvature of the plot for polarizer 2 corresponding to the minimal intensity. The plot for polarizer 2 corresponding to the maximal intensity is a straight line. We suppose the translation coefficient D_T is dominant, when we have a highest value of intensity. In that case only the translational tensor D_T would be observed.

$$D_T = \begin{pmatrix} D_\perp & & \\ & D_\perp & \\ & & D_\parallel \end{pmatrix}$$

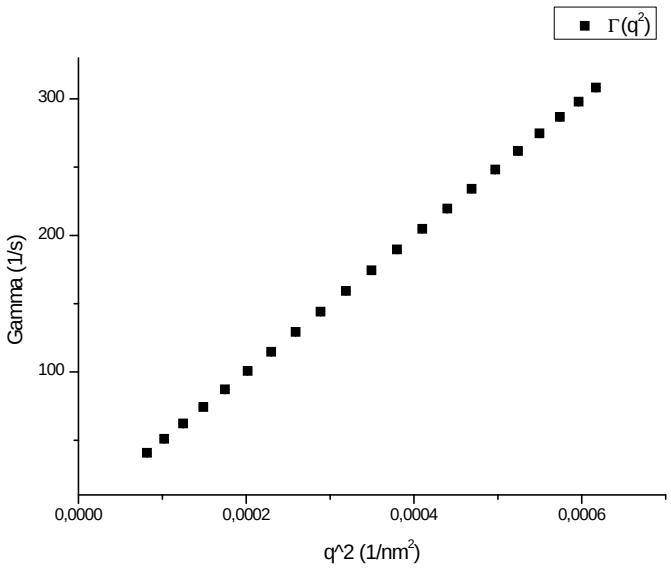

Figure 18: Plot of equation 7 in the first order of approximation

So the curvature of the plot corresponding to the minimal intensity could be explained by the influence of the rotational coefficient D_r. To verify this we tried to plot the equation 7 in the first order of approximation. This procedure did not work, so we could not get expect any results (see Fig. 18).

The next step would be to try higher order of approximation. We still need time to implement the theory and there is still some work in progress.

6 Acknowledgements

We would like to gratefully acknowledge all the people who have been supporting us throughout the whole period spent at DESY ie Christian Gutt, Birgit Fischer, Fabian Westermeier, Wojciech Roseker, Jan Perlich and Ulla Vainio. We really appreciate your help and everything what we could learn from you. The time spent in HASYLAB was both very enjoyable and effectively spent.

References

[1] Jens Als-Nielsen, Des McMorrow.*Elements of Modern X-Ray Physics.*John Wiley & Sons Ltd,2001

[2] Bruce J. Berne, Robert Pecora.*Dynamic Light Scattering. With Applications to Chemistry, Biology, and Physics.*DOVER PUBLICATION INC, 2000

[3] John M. Stone.*Radiation an Optics. An Introduction to the Classical Theory.*McGraw-Hill Book Company Inc,1963

[4] Masataka Ozaki, Stanka Kratohvil, Egon Matijevic.*Formation of Monodispersed Spindle-Type Hematite Particles.*Department of Chemistry and Institute of Colloid and Surface Science, Clarkson University,1984